Highly-Metallized Phosphonium Polyelectrolytes

SCHOLARONE™
Manuscripts

Chemical Communications ChemComm

Communication

Highly-Metallized Phosphonium Polyelectrolytes†

Amir Rabiee Kenaree,*[a] Bradley M. Berven,[a,b] Paul J. Ragogna,*[a] and Joe B. Gilroy*[a]

The synthesis and characterization of a novel class of highly-metallized, redox-active polyelectrolytes that employ phosphorus as a scaffold for the installation of transition metals is described. Pyrolysis of thin films of the title polyelectrolytes resulted in the production of magnetite crystallites and ill-defined carbon-, phosphorus- and oxygen-rich phases in char yields of nearly 50%.

Metallopolymers (or metal-containing polymers) have emerged over the past two decades as a versatile new class of (multi)functional materials.[1,2] These materials, which include main-chain and side-chain architectures, combine the processability of polymers and the highly desirable properties (*e.g.*, redox and catalytic activity, magnetic, light-absorbing) of transition metals. They have received significant attention, for example, as precursors to nanostructured materials,[3] the functional component of redox-active capsules[4] and photonic crystal displays,[5] photoactive materials in solar cells,[6] and antimicrobial surfaces.[7]

By exploiting the chemistry of phosphorus as part of several different synthetic strategies, a promising subclass of metallopolymers has been established.[8] For example, main-chain poly(ferrocenylphosphine)s (*e.g.*, **1**) have been produced by the ring-opening polymerization of strained [1]phosphaferrocenophanes,[9] while a unique migration-insertion polymerization mechanism has been used to produce poly(cyclopentadienylcarbonyldiphenyl-phosphinobutanoyliron)s (*e.g.*, **2**).[10] Block copolymers incorporating a side-chain metallopolymer block based on poly(phosphaalkene)s (*e.g.*, **3**) have been realized through a sequential anionic polymerization / metal-coordination strategy before they were self-assembled into micelles with a gold core.[11]
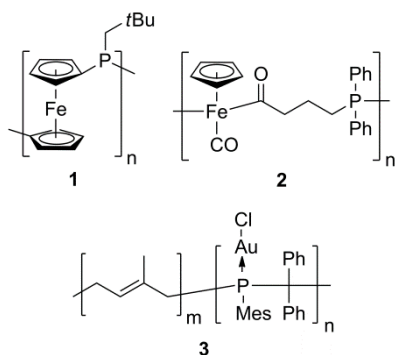
Although advances towards phosphorus-containing metallopolymers have been impressive, examples possessing more than one metal per polymer repeating unit remain elusive. Herein we report a strategy for the synthesis and characterization of highly-metallized phosphonium polyelectrolytes bearing three ferrocenes per repeating unit starting from phosphine gas.

Primary, secondary, and tertiary phosphines **4a–c** were synthesized in one pot via the radical-catalyzed hydrophosphination of vinylferrocene (Scheme 1). Our best results were obtained when the reaction was conducted in a stepwise fashion, keeping the concentration of azobisisobutyronitrile (AIBN) and vinylferrocene low relative to phosphine gas. Phosphines **4a–c**, which are air- and moisture-stable in the solid-state,[12] were isolated by column chromatography on silica gel using a gradient solvent strategy in 20%, 31%, and 27% yield respectively. It is worth noting that the primary and secondary phosphines recovered from the column could be further converted to tertiary phosphine by the addition of AIBN and vinylferrocene when desired.
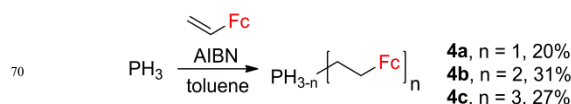
Scheme 1 Synthesis of ferrocene-substituted phosphines **4a–c**.

The solid-state structures of phosphines **4a–c** were determined by single crystal X-ray crystallography (Fig. 1), while multinuclear NMR spectroscopy data were consistent with the proposed structures of **4a** (^{31}P NMR: t, $^1J_{PH}$ = 196 Hz, –137.1 ppm), **4b** (^{31}P NMR: d, $^1J_{PH}$ = 201 Hz, –68.8 ppm), and **4c** (^{31}P NMR: s, –27.9 ppm) in solution (Fig. 2 and S1–S5). For each phosphine, the solid-state structures confirmed that the ferrocene groups are separated from the phosphorus atom by an ethylene spacer [C-C bond lengths 1.50(2)–1.538(7) Å; P-C bond lengths 1.843(1)–1.93(1) Å], confirming the proposed reaction pathway

Tertiary phosphine **4c** was used to produce the target phosphonium polyelectrolytes according to Scheme 2. Quaternization of tertiary phosphine **4c** via reaction with 3-chloro-1-propanol led to the formation of ferrocene-substituted phosphonium chloride salt **5a** as a fine yellow powder in 88% yield (Fig. S6–S8). Ion exchange using sodium tetrafluoroborate yielded microcrystalline phosphonium tetrafluoroborate salt **5b** (Fig. S9–S12). The solid-state structure of **5b** confirmed the
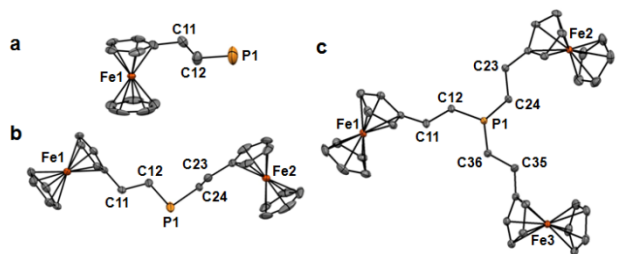
Fig. 1 Solid-state structures of phosphines (a) **4a**, (b) **4b**, and (c) **4c**. Thermal ellipsoids shown at 50% probability level. Hydrogen atoms removed for clarity. Selected bond lengths (Å) for **4a**: P1-C12 1.884(6), C11-C12 1.515(8); **4b**: P1-C12 1.853(6), P1-C24 1.93(1), C11-C12 1.538(7), C23-C24 1.50(2); **4c**: P1-C12 1.843(1), P1-C24 1.853(1), P1-C36 1.855(1), C11-C12 1.537(2), C23-C24 1.533(1), C35-C36 1.533(2). Selected bond angles (°) for **4b**: C12-P1-C24 99.0(4); **4c**: C12-P1-C24 100.34(6), C12-P1-C36 99.26(6), C24-P1-C36 99.44(5).
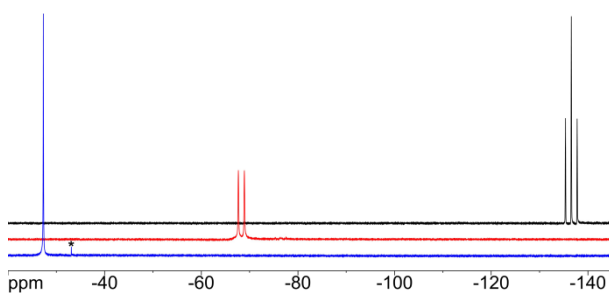

Fig. 2 Proton coupled ^{31}P NMR spectra of phosphines **4a** (black), **4b** (red), and **4c** (blue) in CDCl₃. The signal marked with an asterisk in the spectrum of **4c** has been identified as the mono α-addition product, commonly observed in considerable quantities as a byproduct in the synthesis of phosphines by the mechanism employed.

proposed structure and the presence of a nearly tetrahedral geometry at phosphorus (Fig. S13, Table S1).

Polymerizable phosphonium triflate salt **6** was synthesized in two steps in 89% yield (Scheme 2, Fig. 3 and S14–S16). Esterification of the alcohol group in **5a** was accomplished by reacting it with methacryloyl chloride in the presence of triethylamine under anhydrous conditions. The chloride counter anion was exchanged for a trifluoromethanesulfonate (triflate) anion to overcome the tendency of the phosphonium chloride salts encountered during this study to decompose via an unidentified decomposition pathway in solution when exposed to air.[13] Phosphonium triflate **6** is air- and moisture-stable and has significantly enhanced solubility in organic solvents compared to its chloride analog. The latter trait is highly desirable for further polymerization chemistry where poor solubility can be problematic.

Inspired by the work of Endo,[14] Gin,[15] Long,[16] and others,[17] polyelectrolytes **7a–c** were produced via a free radical polymerization mechanism using AIBN as a thermally-activated initiator. Three polymerization reactions were conducted by first combining monomer **6** and 0.01 (1.0 g monomer mL⁻¹), 0.005 (0.75 g monomer mL⁻¹), and 0.0033 (0.50 g monomer mL⁻¹) molar equivalents of AIBN in THF. Each solution was subjected to three freeze-pump-thaw cycles, before heating at 75 °C for 17, 25, and 32 h, respectively. Polyelectrolytes **7a–c** were isolated in 70%, 79%, and 75% yields after purification by duplicate
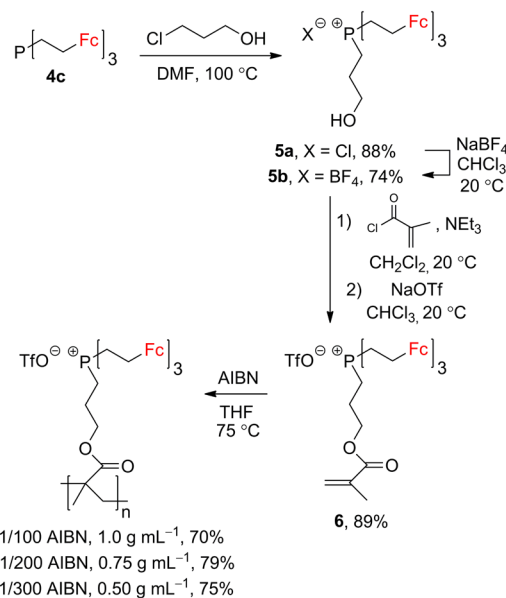
Scheme 2 Synthesis of ferrocene-substituted phosphonium polyelectrolytes **7a–c**. TfO⁻ = trifluoromethanesulfonate (triflate) anion.

precipitation of dichloromethane solutions into benzene and pentane (Fig. 3 and S17–S24, Table 1). ^{1}H NMR spectroscopy confirmed conversion of monomer **6** to polyelectrolytes **7a–c** as the signals attributed to the alkene functionality disappeared (δ 6.16 and 5.66) and new signals assigned to the saturated hydrocarbon backbone appeared (δ 3.00–0.50) in the spectrum of polyelectrolyte **7b** (Fig. 3). The ^{1}H NMR spectra of **7a–c** were very broad, further supporting the proposed polyelectrolyte structures.

By adapting a methodology developed by the Matyjaszewski group,[18] gel permeation chromatography experiments were used to study the molecular weight distributions of polyelectrolytes **7a–c**. These studies confirmed the high molecular weight nature of **7a–c** (M_w = 79,000–118,200 Da, PDI = 2.34–2.74, vs. poly(methyl methacrylate) (PMMA) standards; (Tables 1 and S2 and Fig. S25). Triple detection GPC studies gave molecular weights 3 to 4 times larger than the conventional calibration
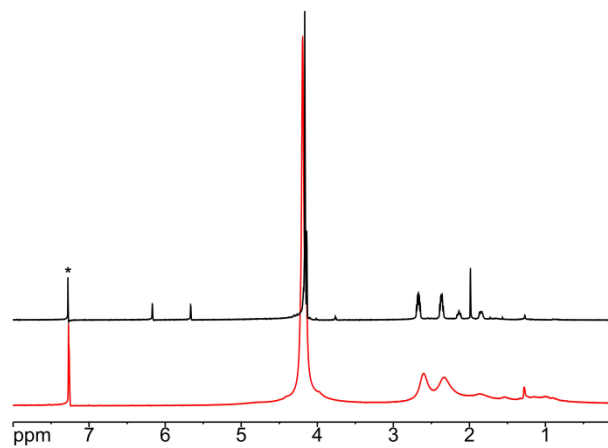

Fig. 3 ^{1}H NMR spectra of monomer **6** (black) and polyelectrolyte **7b** (red) in CDCl₃. The asterisk denotes residual CHCl₃ signals.

studies (Table S3), with the discrepancy likely arising due to size enhancement associated with the non-coordinating triflate anions employed in this study. The trends in molecular weight data were consistent with the free radical polymerization mechanism employed, and revealed that both concentration and monomer:initiator ratio influenced the molecular weights of the polyelectrolytes isolated in an uncontrolled fashion.

Each of the compounds reported in this study, including polyelectrolytes **7a–c** exhibit properties consistent with the presence of ferrocene(s) in solution (Table 1). Their UV-vis spectra exhibit maximum absorption at wavelengths (λ_{max}) of *ca.* 440 nm. Their cyclic voltammograms are comprised of reversible oxidation waves at potentials ($E_{ox}°$) between −10 and 5 mV relative to the ferrocene/ferrocenium redox couple (Fig. 4 and S26–S31). In each case, the current response observed corresponded to one electron for each ferrocene group present. Secondary and tertiary phosphines **4b** and **4c** also exhibited an irreversible oxidation at −95 and −150 mV respectively, which we assign to the oxidation of phosphorus in these electron-rich phosphines.
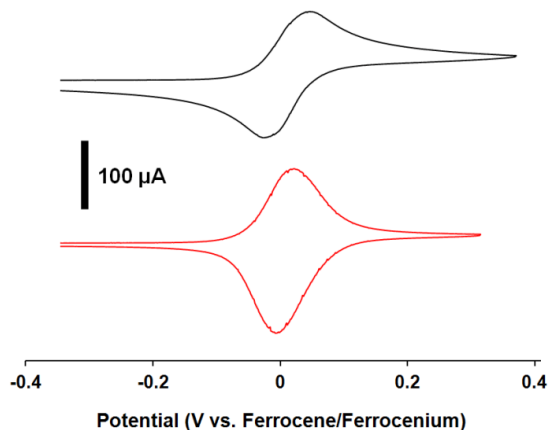

Fig. 4 Cyclic voltammograms of ferrocene-substituted monomer **6** (black) and polyelectrolyte **7b** (red) recorded at 250 mV s^{-1} in 1 mM solutions of 2:1 dichloromethane:acetonitrile containing 0.1 M tetrabutylammonium triflate as supporting electrolyte.

Table 1 Characterization data for compounds **4–7**.

	^{31}P NMR shift (ppm)^a	$E_{ox}°$ (mV vs Fc/Fc$^+$)^b	M$_w$ (Da), PDI^d	R$_h$ (nm)^e
4a	−137.1	−10	-	-
4b	−68.8	−10 (−95)$^{[c]}$	-	-
4c	−27.9	−10 (−150)$^{[c]}$	-	-
5a	32.6	−20	-	-
6	31.9	5	-	-
7a	31.8	0	118,200, 2.74	8.9
7b	31.8	0	78,900, 2.44	8.5
7c	31.9	0	105,700, 2.34	8.6

^{a}Recorded in CDCl$_3$ against triphenylphosphine internal standard. ^{b} Recorded at 250 mV s^{-1} in 1 mM solutions of 2:1 dichloromethane:acetonitrile containing 0.1 M tetrabutyl-ammonium triflate as supporting electrolyte. ^{c}Anodic potential of phosphorus oxidation shown in brackets. ^{d}Determined by conventional calibration GPC vs. PMMA standards. ^{e}Determined by triple detection GPC (right-angle light scattering).

Differential scanning calorimetry studies revealed glass transition temperatures of 108 °C for **7a–c** (Fig. S32–S34).

Thermal gravimetric analysis confirmed their exceptional thermal stability, as **7a–c** all reached 310 °C before significant mass loss was observed. After the onset of decomposition, degradation ocurred in a single smooth step, before the masses plateaued above *ca.* 500 °C (Fig. 5a and S35–S36). The high char yields of ~46% observed for polyelectrolytes **7a–c**, which may result from the low volatility of the ionic compounds generated during decomposition, prompted us to conduct preliminary studies of their pyrolysis behavior.

A thin film of polyelectrolyte **7b** was prepared by spin coating a 80 mg mL^{-1} 3:2 chlorobenzene:chloroform solution onto a freshly cleaned silicon wafer. The film was dried *in vacuo* for 16 h at 50 °C before it was heated to 800 °C at a rate of 10 °C min^{-1} and held at that temperature for an additional 2 h under a steady flow of nitrogen. Upon cooling to room temperature at a rate of 10 °C min^{-1} the pyrolyzed film was exposed to air and analyzed by scanning electron microscopy (SEM) (Fig. 5b and S37–S40). The resulting images and elemental mapping/analysis experiments revealed a mixture of magnetite (Fe$_3$O$_4$) crystallites and a carbon, phosphorus, and oxygen containing phase. Crucially, a significant quantity of the iron within the polyelectrolytes appears to be retained upon pyrolysis, illustrating the promise of this new class of highly-metallized polyelectrolytes as precursors to functional metal-rich ceramics and / or nanoparticles.
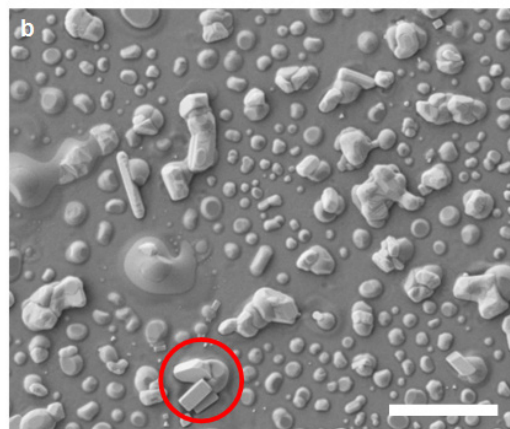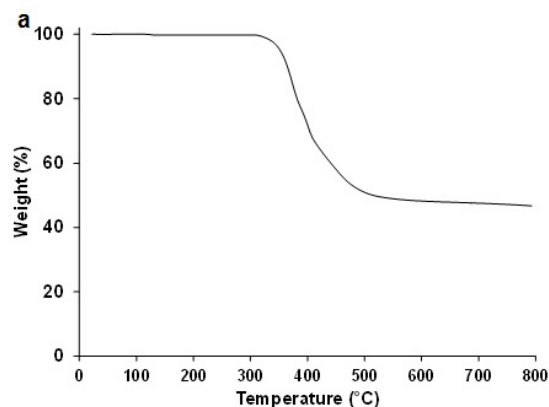

Fig. 5 (a) TGA trace for polyelectrolyte **7b**, and (b) SEM image of the nanostructures produced by heating a thin film of polyelectrolyte **7b** at 800 °C for 2 h under a flow of N$_2$ gas. Representative Fe$_3$O$_4$ crystallites highlighted by red circle. Scale bar = 1 μm. See supporting information for elemental mapping and analysis data.

In conclusion, through the use of a novel and unique approach we have synthesized the first examples of metal-containing phosphonium polyelectrolytes starting from phosphine gas. The polyelectrolytes were shown to be redox-active, due to the presence of ferrocene groups, and their pyrolysis led to the formation of iron-rich nanoparticles and carbon-, phosphorus-, and oxygen-rich phases in high char yields (~46%). Moving forward, the stability of the phosphines isolated during this work will allow us to apply the synthetic methods developed in a modular fashion towards the synthesis of a wide range of functional metal-containing polyelectrolytes. Specifically, polyelectrolytes based on mixed metallocene architectures (metal = Fe, Co, and Ru) will be targeted with a view of realizing alloyed nanoparticles with unusual composition and function.

Notes and references

[a] Department of Chemistry and the Centre for Advanced Materials and Biomaterials Research (CAMBR), The University of Western Ontario, 1151 Richmond St. N., London, Ontario, Canada, N6A 5B7. Fax: +1-519-661-3022; Tel: +1-519-661-2111 ext. 81561; E-mail: pragogna@uwo.ca, joe.gilroy@uwo.ca.

[b] Current Address: 3M Canada, 1840 Oxford Street, London, Ontario, Canada, N5V 3R6.

1 Reviews: (a) V. Marin, E. Holder, R. Hoogenboom and U. S. Schubert, *Chem. Soc. Rev.*, 2007, **36**, 618–635; (b) R. Shunmugam and G. N. Tew, *Macromol. Rapid Commun.*, 2008, **29**, 1355–1362; (c) G. R. Whittell, M. D. Hager, U. S. Schubert and I. Manners, *Nat. Mater.*, 2011, **10**, 176–188; (d) C. G. Hardy, L. Ren, J. Zhang and C. Tang, *Isr. J. Chem.*, 2012, **52**, 230–245.

2 Selected examples: (a) T. J. O'Sullivan, B. Djukic, P. A. Dube, and M. T. Lemaire, *Chem. Commun.* 2009, 1903–1905; (b) B. Bagh, J. B. Gilroy, A. Staubitz and J. Müller, *J. Am. Chem. Soc.*, 2010, **132**, 1794–1795; (c) C. Ulbricht, C. R. Becer, A. Winter and U. S. Schubert, *Macromol. Rapid Commun.*, 2010, **31**, 827–833; (d) C. Cui, J. Heilmann-Brohl, A. Sánchez Perucha, M. D. Thomson, H. G. Roskos, M. Wagner and F. Jäkle, *Macromolecules*, 2010, **43**, 5256–5261; (e) P. Chadha and P. J. Ragogna, *Chem. Commun.*, 2011, **47**, 5301–5303; (f) J. B. Gilroy, S. K. Patra, J. M. Mitchels, M. A. Winnik and I. Manners, *Angew. Chem. Int. Ed.*, 2011, **50**, 5851–5855; (g) L. Ren, J. Zhang, X. Bai, C. G. Hardy, K. D. Shimizu and C. Tang, *Chem. Sci.*, 2012, **3**, 580–583; (h) H. Braunschweig, T. Dellermann, R. D. Dewhurst, J. Mies, K. Radacki, S. Stellwag-Konertz, M. Wagner and A. Vargas, *Organometallics*, 2014, **33**, 1536–1539; (i) S. Baljak, A. D. Russell, S. C. Binding, M. F. Haddow, D. O'Hare and I. Manners, *J. Am. Chem. Soc.*, 2014, **136**, 5864–5867; (j) Y. Wang, A. Rapakousiou and D. Astruc, *Macromolecules*, 2014, **47**, 3767–3774.

3 Selected examples: (a) M. J. MacLachlan, M. Ginzburg, N. Coombs, T. W. Coyle, N. P. Raju, J. E. Greedan, G. A. Ozin and I. Manners, *Science*, 2000, **287**, 1460–1463; (b) Z. M. Al-Badri, R. R. Maddikeri, Y. Zha, H. D. Thaker, P. Dobriyal, R. Shunmugam, T. P. Russell and G. N. Tew, *Nat. Commun.*, 2011, **2**, 482; (c) Q. Dong, G. Li, C.-L. Ho, M. Faisal, C.-W. Leung, P. W.-T. Pong, K. Liu, B.-Z. Tang, I. Manners and W.-Y. Wong, *Adv. Mater.*, 2012, **24**, 1034–1040; (d) J. Kamcev, D. S. Germack, D. Nykypanchuk, R. B. Grubbs, C.-Y. Nam and C. T. Black, *ACS Nano*, 2013, **7**, 339–346.

4 (a) Y. Ma, W.-F. Dong, M. A. Hempenius, H. Möhwald and G. J. Vancso, *Nat. Mater.*, 2006, **5**, 724–729; (b) R. H. Staff, M. Gallei, M. Mazurowski, M. Rehahn, R. Berger, K. Landfester and D. Crespy, *ACS Nano*, 2012, **6**, 9042–9049.

5 A. C. Arsenault, D. P. Puzzo, I. Manners and G. A. Ozin, *Nat. Photonics*, 2007, **1**, 468–472.

6 W.-Y. Wong, X.-Z. Wang, Z. He, A. B. Djurišić, C.-T. Yip, K.-Y. Cheung, H. Wang, C. S. K. Mak and W.-K. Chan, *Nat. Mater.*, 2007, **6**, 521–527.

7 J. Zhang, Y. P. Chen, K. P. Miller, M. S. Ganewatta, M. Bam, Y. Yan, M. Nagarkatti, A. W. Decho and C. Tang, *J. Am. Chem. Soc.*, 2014, **136**, 4873–4876.

8 Selected examples: (a) H. R. Allcock, J. A. Dodge, I. Manners and G. H. Riding, *J. Am. Chem. Soc.*, 1991, **113**, 9596–9603; (b) C. Díaz and M. L. Valenzuela, *Macromolecules*, 2006, **39**, 103–111; (c) M. Sebastian, M. Hissler, C. Fave, J. Rault-Berthelot, C. Odin and R. Réau, *Angew. Chem. Int. Ed.*, 2006, **45**, 6152–6155; (d) E. W. Ainscough, H. R. Allcock, A. M. Brodie, K. C. Gordon, M. D. Hindenlang, R. Horvath and C. A. Otter, *Eur. J. Inorg. Chem.*, 2011, 3691–3704; (e) G. A. Carriedo, S. López, S. Suárez-Suárez, D. Presa-Soto and A. Presa-Soto, *Eur. J. Inorg. Chem.*, 2011, 1442–1447.

9 Selected examples: (a) C. H. Honeyman, D. A. Foucher, F. Y. Dahmen, R. Rulkens, A. J. Lough and I. Manners, *Organometallics*, 1995, **14**, 5503–5512; (b) T. J. Peckham, J. A. Massey, C. H. Honeyman and I. Manners, *Macromolecules*, 1999, **32**, 2830–2837; (c) T. Mizuta, Y. Imamura and K. Miyoshi, *J. Am. Chem. Soc.*, 2003, **125**, 2068–2069; (d) S. K. Patra, G. R. Whittell, S. Nagiah, C.-L. Ho, W.-Y. Wong and I. Manners, *Chem. Eur. J.*, 2010, **16**, 3240–3250.

10 (a) X. Wang, K. Cao, Y. Liu, B. Tsang and S. Liew, *J. Am. Chem. Soc.*, 2013, **135**, 3399–3402; (b) K. Cao, B. Tsang, Y. Liu, D. Chelladural, W. P. Power and X. Wang, *Organometallics*, 2014, **33**, 531–539.

11 K. J. T. Noonan, B. H. Gillon, V. Cappello and D. P. Gates, *J. Am. Chem. Soc.*, 2008, **130**, 12876–12877.

12 (a) W. Henderson and S. R. Alley, *J. Organomet. Chem.*, 2002, **656**, 120–128; (b) B. Stewart, A. Harriman and L. J. Higham, *Organometallics*, 2011, **30**, 5338–5343.

13 Decomposition of ferrocene-containing phosphonium salts may occur due to the generation of HCl upon exposure to air.

14 Selected examples: (a) A. Kanazawa, T. Ikeda and T. Endo, *J. Polym. Sci., Part A: Polym. Chem.*, 1993, **31**, 335–343; (b) A. Kanazawa, T. Ikeda and T. Endo, *J. Polym. Sci., Part A: Polym. Chem.*, 1993, **31**, 1467–1472; (c) A. Kanazawa, T. Ikeda and T. Endo, *J. Polym. Sci., Part A: Polym. Chem.*, 1993, **31**, 3003–3011; (d) A. Kanazawa, T. Ikeda and T. Endo, *J. Appl. Polym. Sci.*, 1994, **53**, 1237–1244.

15 E. S. Hatakeyama, H. Ju, C. J. Gabriel, J. L. Lohr, J. E. Bara, R. D. Noble, B. D. Freeman and D. L. Gin, *J. Membr. Sci.*, 2009, **330**, 104–116.

16 (a) S. Cheng, F. L. Beyer, B. D. Mather, R. B. Moore and T. E. Long, *Macromolecules*, 2011, **44**, 6509–6517; (b) S. Cheng, M. Zhang, T. Wu, S. T. Hemp, B. D. Mather, R. B. Moore and T. E. Long, *J. Polym. Sci., Part A: Polym. Chem.*, 2012, **50**, 166–173; (c) S. T. Hemp, M. H. Allen, Jr., M. D. Green and T. E. Long, *Biomacromolecules*, 2012, **13**, 231–238.

17 Selected examples: (a) R. Wang and A. B. Lowe, *J. Polym. Sci., Part A: Polym. Chem.*, 2007, **45**, 2468–2483; (b) K. J. T. Noonan, K. M. Hugar, H. A. Kostalik, E. B. Lobkovsky, H. D. Abruna and G. W. Coates, *J. Am. Chem. Soc.*, 2012, **134**, 18161–18164.

18 H. He, M. Zhong, B. Adzima, D. Luebke, H. Nulwala and K. Matyjaszewski, *J. Am. Chem. Soc.*, 2013, **135**, 4227–4230.